

CENTER FOR SPACE RESEARCH

The University of Texas at Austin  
Austin, Texas

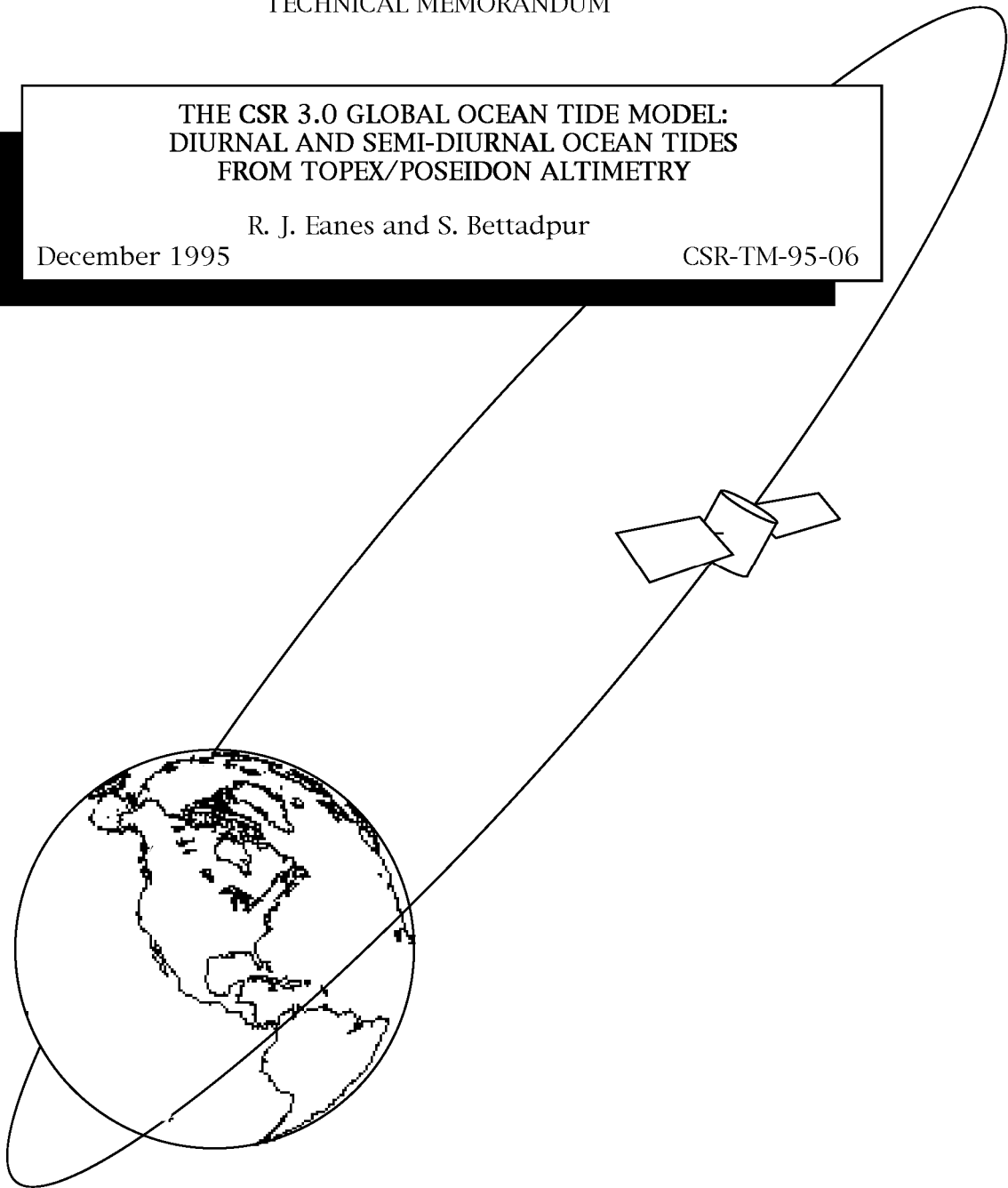
TECHNICAL MEMORANDUM

THE CSR 3.0 GLOBAL OCEAN TIDE MODEL:  
DIURNAL AND SEMI-DIURNAL OCEAN TIDES  
FROM TOPEX/POSEIDON ALTIMETRY

R. J. Eanes and S. Bettadpur

December 1995

CSR-TM-95-06



**THE CSR 3.0 GLOBAL OCEAN TIDE MODEL:  
DIURNAL AND SEMI-DIURNAL OCEAN TIDES  
FROM TOPEX/POSEIDON ALTIMETRY**

by

Richard J. Eanes and Srinivas Bettadpur

Center for Space Research  
The University of Texas at Austin

December 1996

CSR-TM-95-06

This work was supported by  
NASA Contract JPL/CIT #956689

Center for Space Research  
The University of Texas at Austin  
Austin, Texas 78712

Principal Investigator:  
Byron D. Tapley

**THE CSR 3.0 GLOBAL OCEAN TIDE MODEL:  
DIURNAL AND SEMI-DIURNAL OCEAN TIDES  
FROM TOPEX/POSEIDON ALTIMETRY**

## **1. INTRODUCTION**

The successful launch and operation of TOPEX/POSEIDON (T/P), a joint NASA/ESA radar altimeter mission, has proven to be a boon for a wide range of oceanography applications. High accuracy measurements of the height of the T/P satellite over the instantaneous ocean surface, coupled with highly accurate determination of the geocentric distance to the satellite using sophisticated orbit determination techniques and models, has led to several advances in the modeling of features and phenomena over the global oceans. The use of this data for mapping of the Mean Sea Level, Dynamic Sea Surface Topography, Ocean Tides and other oceanographic phenomena is well documented (JGR Vol. 90 (C12), 1994).

The models for global ocean tides have seen significant improvements, beginning from the models of Schwiderski (1983) which used long spans of globally distributed tide gauge data; through the Cartwright and Ray (1990) model (C&R91 Model), which used three years of altimeter data from Geosat; and finally to several models derived from the T/P altimeter data (e.g. Desai and Wahr (D&W95) Model (1995)).

In this report, we provide an outline of the theoretical basis, the data processing and the error assessment results from the development of the ocean tide **Model CSR 3.0**. This model was estimated from T/P altimeter normal points over a span of 2.4 years (first 89 cycles), using the response method developed by Munk and Cartwright (1966). The reference model adopted was the FES94.1 (Le Provost, 1994), and corrections to the ocean tide orthoweights in the Diurnal and Semi-diurnal band, among other parameters, were estimated from T/P altimeter residuals with respect to the reference model. As is evident, there are several principal topics of discussion in this report, namely

- a) the mathematical model for the ocean tide itself;
- b) the reference model FES 94.1, residuals with respect to which were used to estimate the model CSR 3.0;
- c) the pre-processing and corrections applied to the T/P satellite altimeter measurements;
- d) parametrization of the corrections to the reference ocean tides;
- e) the least squares problem formulation, solution and post-processing; and finally
- f) the error analysis and accuracy assessments of the final model.

Each of these topics are discussed in succession in the following sections of this report.

## 2. THEORETICAL MODELS

Since a satellite altimeter measures the height of the instantaneous ocean surface relative to a reference ellipsoid, we get a direct measurement of the geocentric or the so-called altimetric tide, denoted at a given latitude  $\phi$  and longitude  $\lambda$  at any epoch  $t$  by  $\zeta^a(\phi, \lambda; t)$ . This altimetric tide is related to the true, or bottom-relative ocean tide  $\zeta(\phi, \lambda; t)$  by

$$\zeta^o(\phi, \lambda; t) = \zeta^a(\phi, \lambda; t) - \zeta^b(\phi, \lambda; t) = \zeta(\phi, \lambda; t) + \zeta^l(\phi, \lambda; t) \quad (1)$$

where  $\zeta^b$  is solid or the body-tide, and  $\zeta^l$  is the load tide. The difference between the altimetric and the load tides will be called the elastic ocean tide (Callahan 1993), denoted by  $\zeta^o$ . While the T/P altimeter makes measurements of the altimetric tide, we choose to treat  $\zeta^o$  as the observable quantity for two reasons. Firstly, the response of the solid Earth to the tidal potential is, except for the Free Core Nutation (FCN) effects, well understood and accurately modeled at the Diurnal and Semi-diurnal frequencies, so that the body tides may be treated as a correction applied to the altimeter data. Secondly, the spectral nature of ocean tides, including their loading effects, are quite distinct and more complicated than the nature of the solid tides. For these reasons, we chose to club together the bottom relative ocean tide and the ocean load tide into the elastic ocean tide.

The loading deformation due to ocean tides is used in two places in this work. Firstly, the load tides are required to convert the bottom relative reference FES94.1 ocean tide model to the reference elastic ocean tide. Secondly, once the elastic ocean tide is estimated from the T/P data, the final model must be converted to the bottom-relative tide using ocean loads. It is important to emphasize that the two load models were distinct, with the first or the Reference Load Tide model based upon a previous T/P ocean tide model CSR 2.0 (Eanes and Bettadpur, 1994), and the latter computed from a self-consistent analysis of the model CSR 3.0 itself.

The following theory is formulated for the models of the bottom relative tide  $\zeta$ , although it is pointed out that the theory is equally applicable to either the bottom relative tide  $\zeta$  or to the elastic ocean tide  $\zeta^o$ . Such a formulation does not take into account the possible resonant behavior in the load tides at the FCN frequency (Wahr and Sasao, 1981).

## 2.1. The Response Method

The tidal response method, first applied to the analysis of tide gauge data in Munk and Cartwright (1966), is one of the more popular techniques for empirical modeling of ocean tides. The mathematical framework for this method, using the so-called orthoweights, was set out in great detail in Groves and Reynolds (1975). This method was successfully used to develop the C&R91 ocean tide model from Geosat altimeter data, as also the more recent ocean tide models from T/P altimeter data (e.g. Eanes, 1994; Eanes and Bettadpur, 1994; Desai and Wahr, 1995). Our mathematical formulation mirrors that of Groves and Reynolds (1975), Cartwright and Ray (1990), and of Desai and Wahr (1995), so that the details need not be repeated here.

In the response formalism, as set out by Munk and Cartwright (1966), the ocean tide height at each geographical location is expressed as a discrete convolution of the tide generating potential with suitable weights in the time domain. The weights at each time lag are chosen to minimize the error in prediction of tide height at a given location, so that the chosen weights become functions of only the location and time lag; which, along with the tide generating potential, completely determine the tide height at that location. If the tide generating potential is decomposed into its spherical harmonic spatial distribution modulated by time dependent variations in the Long Period, Diurnal and Semi-diurnal species, the tide height then becomes a discrete time convolution between the purely time varying part of the tide generating potential and the spherical harmonic components of the weights. These latter weights are called the Tidal Admittances, as they are also the global frequency response of the ocean tide height to the purely time dependent component of the tidal forcing. The modeling of the tidal admittances also imposes the so-called "credo of smoothness" on the ocean response as a function of frequency over a selected frequency range. From discrete Fourier transforms, it follows that the frequency range is determined by the time lag interval, and the structure of the admittances over this range is determined by the number of time lag steps imposed on the model. For example, for a fixed time lag interval or bandwidth, using no lag intervals implies a constant admittance over the applicable frequency range; using one lag interval implies modeling the admittance as a sinusoidal function of frequency with one complete cycle over the selected bandwidth; and so on. Clearly, greater the number of selected time lags, weaker is the imposition of the "credo of smoothness" over the selected bandwidth.

Groves and Reynolds (1975) proposed a modification to this basic methodology by introducing the so-called orthotides. In this approach, the tides at each location were written as a weighted sum of orthotides, where the weights were again determined to minimize the prediction error at that location. The orthotides, on the other hand, are linear combinations of the time dependent part of the tide generating potential such that their time convolution over a theoretically infinite time interval is zero for distinct frequencies. The "credo of smoothness" is imposed by constructing the orthotides with successively greater number of lags in the linear combinations, so that the orthotides of the lowest orders are the smoothest over the selected bandwidth. The coefficients of such linear combinations, also called the Orthotide Coefficients, are in practice, numerically determined by convolving a large number of tidal harmonics over a suitably large time interval. The weights for the orthotides, as before, remain a function of the geographical location.

The choice of the bandwidth over which the response is modeled depends on the value of the time lag in the convolution. Munk and Cartwright (1966) suggested an interval of 48 hrs, with an implied bandwidth of 0.5 cyc/day. Most of the important Diurnal tides lie within frequencies of 0.8 and 1.1 cyc/day, and the Semi-diurnal tides within 1.75 and 2.05 cyc/day, a bandwidth of 0.3 cyc/day. As a compromise between minimizing the aliasing from tidal harmonics outside this bandwidth, and in imposing the "credo of smoothness" over a sufficiently wide frequency range, the value of 48 hrs was chosen for the time lag, a choice which we use throughout in the succeeding discussion.

## 2.2. The General Response Model

Following this outline of the basic theory, the model for the ocean tide height can be developed as follows. Let the astronomical tide generating potential of degree two be written as (Cartwright and Tayler, 1971)

$$V(\phi, \lambda; t) = g \sum_{m=0}^2 c_2^m(t) W_2^m(\phi, \lambda) \quad (2a)$$

where,

$$c_2^m(t) \equiv a_2^m(t) + i b_2^m(t) = \sum_k H_k e^{-i(\Theta_k + \chi_k)} \quad (2b)$$

and  $W_2^m$  are the surface spherical harmonics of degree two, as defined in Eqs. 10 and 11 in Cartwright and Taylor (1971). In these expressions,  $H_k$  denotes the Cartwright and Taylor amplitudes,  $\chi_k$  denotes the Doodson-Warburg phase factor (McCarthy, 1992), and  $\Theta_k$  denotes tidal argument for the harmonic constituent  $k$ . The summation over the index  $k$  is carried out for all the harmonics arising from each order  $m$  of the tide generating potential. Each of the tidal arguments can be written as

$$\Theta_k(t) = k_1\tau + (k_2-5)s + (k_3-5)h + (k_4-5)p + (k_5-5)N' + (k_6-5)p_s(2c)$$

where  $k_1$  is equal to  $m$  in Eq. 2a, and where the astronomical arguments have the usual meaning as defined in (McCarthy, 1992).

In the expression for the tidal potential, the degree and order are explicitly indicated by the subscript 2 and the superscript  $m$ . However, there is little possibility of confusion if both the subscript and the superscript are dropped from the future expressions, with the understanding that each such expression applies separately for each order  $m$ , or equivalently, for each tidal species.

If  $n$  denotes the "order" of the orthotide (Groves and Reynolds, 1975), and if  $u_n$  and  $v_n$  denote the weights for that orthotide, (which will be determined from the observation data at each geographic location), then the tide height at any point can be written as

$$\zeta(t) = \sum_{n: \text{even}}^{\infty} [ u_n P_n(t) + v_n Q_n(t) ] \quad (3a)$$

where the orthotides  $P_n$  and  $Q_n$  are written as

$$P_n = \sum_{s=0}^{i_n} U_{n,s} a_s^+(t) + V_{n,s} b_s^-(t) \quad (3b)$$

$$Q_n = \sum_{s=0}^{i_n} U_{n,s} b_s^+(t) - V_{n,s} a_s^-(t) \quad (3c)$$

and where

$$a_s^\pm(t) = a(t + s \Delta t) \pm a(t - s \Delta t) \quad (3d)$$

$$b_s^\pm(t) = b(t + s \Delta t) \pm b(t - s \Delta t) \quad (3e)$$

In the sequel, we will refer to the orthotide weights  $u_i$  and  $v_i$  as the **orthoweights** of the tide for a particular species. In these expression,  $\Delta t$  is the aforementioned time

lag for the convolution. The constants  $U_{n,s}$  and  $V_{n,s}$  are the Orthotide Coefficients of order  $n$  and lag  $s$ , and are tabulated to a high order in Table 2 in Groves and Reynolds (1975).

The reduction in the number of non-zero orthotide coefficients in the Eqs. 3 follows from the imposition of symmetries between the even and odd order orthotides and between terms of positive and negative lag, as discussed in Desai and Wahr (1995). The tide model thus requires only orthotides of even orders, each of which have lags determined by the index range

$$i_n = [ ( n + 6 ) / 4 ] - 1 \quad (4)$$

except for the zeroth order orthotide, when  $i_n = 0$ . Finally, recall that the expressions in Eq. 3 apply to the tidal species for which the expressions  $a(t)$  and  $b(t)$  are being evaluated, so that the total height will be the sum of the heights over all the tidal species.

### 2.3. The Adopted Response Model

While Eq. 3 gives the general form for the ocean tide height for each species, the model adopted in this work was limited to the first three significant orders. In this case, for each species, the tide height is given by

$$\zeta(\phi, \lambda; t) = \sum_{n: \text{even}}^4 [ u_n(\phi, \lambda) P_n(t) + v_n(\phi, \lambda) Q_n(t) ] \quad (5)$$

where the orthotides are computed as

$$P_0 = U_{0,0} a(t) \quad , \quad Q_0 = U_{0,0} b(t) \quad (6a)$$

$$P_2 = U_{2,0} a(t) + U_{2,1} a_1^+(t) \quad , \quad (6b)$$

$$Q_2 = U_{2,0} b(t) + U_{2,1} b_1^+(t)$$

and

$$P_4 = U_{4,0} a(t) + U_{4,1} a_1^+(t) + V_{4,1} b_1^-(t) \quad , \quad (6c)$$

$$Q_4 = U_{4,0} b(t) + U_{4,1} b_1^+(t) - V_{4,1} a_1^-(t)$$

The coefficients  $U_{i,j}$  and  $V_{i,j}$  were taken from Groves and Reynolds (1975), and the non-zero values are tabulated here in Table 1. Note that for each geographic location,

six orthoweights, denoted by  $u_i$  and  $v_i$  for  $i=0,2,4$  are to be estimated for each species from the data.

**Table 1:** Values of the orthotide coefficients, from Groves and Reynolds (1975). Units are  $cm^{-1}$ .

Symbol	Diurnal Species	Semi-diurnal Species
$U_{0,0}$	0.0298	0.0200
$U_{2,0}$	0.1408	0.0905
$U_{2,1}$	-0.0805	-0.0638
$U_{4,0}$	0.6002	0.3476
$U_{4,1}$	-0.3025	-0.1645
$V_{4,1}$	0.1517	0.0923

The expression for the tide height for each species can also be set explicitly in the form of a discrete convolution between the time dependent part and the other factors. First we note that if

$$z_i(\phi, \lambda) \equiv u_i(\phi, \lambda) - i v_i(\phi, \lambda) \quad (7a)$$

and

$$S_i(t) = P_i(t) + i Q_i(t) \quad (7b)$$

then for each species at a given location,

$$\zeta(\phi, \lambda; t) = \text{Re} \cdot \left[ \sum_{i: \text{even}}^4 z_i(\phi, \lambda) S_i(t) \right] \quad (8)$$

where  $\text{Re}[\cdot]$  denotes the real part of the complex argument. Furthermore, we have

$$P_0 + i Q_0 = U_{0,0} c(t) \quad (9a)$$

$$P_2 + i Q_2 = U_{2,0} c(t) + U_{2,1} [c(t+\Delta t) + c(t-\Delta t)] \quad (9b)$$

and

$$\begin{aligned} P_4 + i Q_4 = & U_{4,0} c(t) + (U_{4,1} - i V_{4,1}) c(t+\Delta t) \\ & + (U_{4,1} + i V_{4,1}) c(t-\Delta t) \end{aligned} \quad (9c)$$

Factoring out the time dependent part, we can reset the tide height as

$$\zeta(\phi, \lambda; t) = \text{Re} \cdot \left[ \sum_{s=-1}^1 w_s(\phi, \lambda) c(t + s \Delta t) \right] \quad (10)$$

where

$$w_0 = U_{0,0} z_0 + U_{2,0} z_2 + U_{4,0} z_4 \quad (11a)$$

$$w_1 = U_{2,1} z_2 + (U_{4,1} - i V_{4,1}) z_4 \quad (11b)$$

$$w_{-1} = U_{2,1} z_2 + (U_{4,1} + i V_{4,1}) z_4 \quad (11c)$$

The expressions in Eqs. 10 and 11 show that the tide height is being written as a one-step convolution between the tide generating potential and the weights. The tidal admittance, therefore, is a one term sinusoid over the frequency band-width determined by the time lag  $\Delta t$ .

Since the time dependent part at frequency  $k$  has been written as (Eq. 2)

$$c_k(t) = H_k e^{-i(\Theta_k + \chi_k)} \quad (12)$$

we note that for each frequency, the tide height could have been written as

$$\zeta_k(\phi, \lambda; t) = \text{Re} \cdot \left[ H_k e^{-i(\Theta_k + \chi_k)} \sum_{s=-1}^1 w_s(\phi, \lambda) e^{-i \dot{\Theta}_k s \Delta t} \right] \quad (13)$$

so that, by definition, the complex admittance at frequency  $k$  becomes

$$Z_k = X_k + i Y_k = \sum_{s=-1}^1 w_s(\phi, \lambda) e^{-i \dot{\Theta}_k s \Delta t} \quad (14)$$

Separating out explicitly the real and imaginary parts, we have

$$X_k = U_{0,0} u_0 + U_{2,0} u_2 + U_{4,0} u_4 \quad (15a)$$

$$\begin{aligned} &+ 2 (U_{2,1} u_2 + U_{4,1} u_4) \cos \dot{\Theta}_k \Delta t \\ &+ 2 V_{4,1} u_4 \sin \dot{\Theta}_k \Delta t \end{aligned} \quad (15a)$$

$$\begin{aligned} Y_k &= U_{0,0} v_0 + U_{2,0} v_2 + U_{4,0} v_4 \\ &+ 2 (U_{2,1} v_2 + U_{4,1} v_4) \cos \dot{\Theta}_k \Delta t \\ &+ 2 V_{4,1} v_4 \sin \dot{\Theta}_k \Delta t \end{aligned} \quad (15b)$$

As a last step, the real and imaginary parts of the admittance may be converted to the equivalent in-phase and quadrature amplitudes of the tide height. Defining the Greenwich phase (Cartwright and Ray 1991) for each tide by

$$\sigma_k = \Theta_k + \chi_k \quad (16)$$

we write the tide height at each frequency as

$$\zeta_k(\phi, \lambda; t) = H1(\phi, \lambda) \cos \sigma_k + H2(\phi, \lambda) \sin \sigma_k \quad (17)$$

then

$$H1 = (-1)^m H_k X_k(\phi, \lambda) \quad (18a)$$

$$H2 = -(-1)^m H_k Y_k(\phi, \lambda) \quad (18a)$$

where  $m$  is, respectively, 0, 1 and 2 for the Long-period, Diurnal and Semi-diurnal species.

Note that the tide height for each species, whether modeled as in Eq. 5, or as in Eq. 10, requires six parameters. Obviously, the advantage in using the model of Eq. 5 is the numerical stability that follows from the orthotides. Finally, it is pointed out that the model in Eq. 5 is applicable equally to either the bottom relative tide, or to the elastic ocean tide.

### 3. THE REFERENCE TIDE MODEL

From past experience, it has been observed that the altimeter data from T/P altimeter, on its own, is not sufficient to provide good global ocean tide models for two reasons. First, the 66 degree inclination of the TOPEX satellite orbit causes large data gaps at the higher latitudes, making such models non-global. Second, the 2.8 degree nominal ground track separation at the equator reduces the possible resolution of such models, leading to ill-defined ocean tide values within a few hundred kilometers of the coastline.

In an effort to avoid the lack of fine resolution inherent in the T/P satellite coverage, while taking advantage of the high accuracy of the T/P measurements, it was decided to use the T/P altimeter data to make corrections to a high resolution global ocean tide model. For this purpose, the Grenoble FES94.1 hydrodynamical model (Le Provost, 1994) was chosen as the reference. This model is a high resolution harmonic model, obtained by solving the Laplace Tidal Equations using finite element techniques. Maps of global ocean tide height amplitudes are given at the  $Q_1$ ,  $O_1$ ,  $P_1$ ,  $K_1$  frequencies in the Diurnal tidal band, and the  $N_2$ ,  $M_2$ ,  $S_2$ ,  $K_2$  frequencies in the Semi-diurnal bands. The solution is also nominally provided at 5 other frequencies in the Diurnal and Semi-diurnal bands, but these were not used in our procedure as the heights at these frequencies were obtained by interpolating from a linear admittance model imposed upon the eight frequencies listed previously.

While the maps of the Diurnal ocean tides from the Grenoble FES94.1 model were used as provided, Anderson's adjustments to the Grenoble model (Anderson, 1995) were used in the Semi-diurnal tidal band. These latter corrections use the data from the T/P altimeter to correct rather large errors in principally the amplitudes of the  $M_2$  harmonic in the FES94.1 model. The dataset was completed in the Diurnal and Semi-diurnal bands by using Canceil et al. (1995) model for the tides in the Mediterranean.

This reference model provides global maps of the in-phase and quadrature amplitudes of the bottom relative ocean tide height at 8 Diurnal and Semi-diurnal frequencies at half degree grid resolutions. The first step was to convert these to maps of the elastic ocean tide, using the last expression in Eq. 1.

Once the maps of the elastic ocean tides were obtained, a set of reference orthoweights were computed from these maps. The relationship between the in-phase and quadrature amplitudes at each frequency and the corresponding orthoweights for that species are as given in Eqs. 18. Note that the information in each species is available at 4 distinct frequencies. With the in-phase and quadrature components of each tide, this provides 8 pieces of information from which 6 parameters of the orthoweights were estimated for each species.

### 3.1. The Reference Load Tide

In order to convert the bottom relative FES94.1 reference model to the reference elastic ocean tide, an ocean tide loading correction had to be applied. The load tide corrections were derived from a previous T/P based ocean tide model CSR 2.0 (Eanes and Bettadpur, 1994) using the harmonic method.

Note that the ocean tide height is the product of space dependent orthoweights and the time dependent arguments of the tide generating potential. In the response method, the space dependent orthoweights are the same for all frequencies in the same tidal species. Thus the spherical harmonic decomposition of the tide height at each frequency can be computed directly from the spherical harmonic decomposition of the orthoweights for that tidal species. The harmonic method of load tide computation (Ray and Sanchez, 1989) is, in essence, applied directly in the orthoweights domain.

The procedure adopted in computing the reference ocean load tide was as follows. A spherical harmonic decomposition of equi-angular gridded maps of the orthoweights of the CSR 2.0 elastic ocean tide model was obtained using fast Fourier transform techniques (Kim 1995). These coefficients were then scaled with the appropriate load Love numbers  $k_n'$ . The scale factor for the conversion of harmonics at each degree from elastic ocean tide to the load tide was

$$\beta_{nm} = \frac{\alpha_{nm}}{1 + \alpha_{nm}} \quad (19a)$$

$$\alpha_{nm} = 3 \frac{\rho_w}{\rho_e} \frac{h_n'}{(2n + 1)} \quad (19b)$$

where  $\rho_w$  is the density of sea water at 1.025 g/cc, and  $\rho_e$  is the mean solid Earth density at 5.515 g/cc. The Love numbers were obtained by interpolating between the

values tabulated by Farrell (1972). Orthoweights of the load tide for each species were then computed by fast spherical harmonic synthesis. Finally, the addition of the fit orthoweights from the FES94.1 model and the computed load orthoweights from the reference load tide model give the reference orthoweights of the elastic ocean tide model.

#### 4. DATA PRE-PROCESSING AND CORRECTIONS

The T/P altimeter provides high accuracy measurements of the height of the satellite over the instantaneous ocean surface. The TOPEX satellite is in an exact repeat orbit around the Earth, so that the global oceans are sampled once every 9.91 days, with the misclosure between the successive repeat track maintained at less than 1 km. The nominal ground track separation at the equator is approximately 2.8 degrees and the measurements provide coverage of the globe between maximum north and south latitudes of 66 degrees.

The altimeter data from each repeat cycle is provided in the form of the Geophysical Data Records (GDR) (Callahan, 1993) by the Jet Propulsion Laboratory (JPL). The GDR contain the height of the ocean surface above the standard International Reference Ellipsoid. These heights are computed by subtracting the corrected (for sensor, EM-Bias, Ionosphere and Wet/Dry Troposphere effects) altimeter range from the height of the TOPEX satellite above the reference ellipsoid. Also provided in the GDR are the applicable instrument and media corrections, the satellite height over the reference ellipsoid, as well as the suggested (though not applied) geophysical information for the ocean, elastic, load and pole tides, the geoid height and the mean sea surface.

##### 4.1. The Measurement

We first summarize the computation of the measurement residuals used to correct the reference elastic ocean tide model. If  $Y_{ssh}$  denotes the height above the ellipsoid of the instantaneous sea surface as measured by the T/P altimeter, then the residual sea surface height  $y_{obs}$  from which the elastic ocean tides are to be estimated are given by

$$y_{obs} = Y_{ssh} - ( Y_{mss} + Y_b + Y_i ) - Y_r \quad (20)$$

where

$Y_{ssh}$ : is the sea surface height obtained by differencing the satellite height and the corrected altimeter measurement.

$Y_{mss}$ : is the mean sea surface height, which is the sum of the geoidal height and the long period average of the quasi-static mean sea surface topography.

$Y_b$ : denote the body and pole tides.

$Y_i$ : are the Inverted Barometer (IB) corrections.

$Y_r$ : is the reference elastic ocean tide model as described earlier in the last section.

## 4.2. Pre-processing Outline

The altimeter measurement residuals are computed in two steps. In the first step, the high rate (1 Hz) altimeter data from the GDR are verified, edited, smoothed and re-formatted into 10 second normal points. The altimeter measurements are re-synthesized in this stage by adding together the corrected sea surface heights and the POE orbits provided on the GDR. A high frequency component of the mean sea surface (above harmonic degree 70, up to degree 360) is removed from the 1 Hz data before being reduced to 0.1 Hz normal points. The corrections significant for modeling of ocean tides during this stage include the Wet/Dry tropospheric refraction corrections included in the GDR.

In the next step, the altimeter normal points, along with the associated crossover height differences are processed in the University of Texas Orbit Processor software UTOPIA. The orbit for TOPEX is determined almost entirely from the tracking data, an EM-Bias correction is estimated from only the crossover height differences, and an altimeter bias is estimated from the altimeter normal point measurements. Also at this stage, the long wavelength mean sea surface correction is computed from the sum of the degree and order 70 expansion of the JGM-3 geopotential model and a long term mean quasi-static sea surface topography model (Tapley et al., 1994). An IB correction is also applied to the altimeter normal points at this stage. These computations, along with the suggested body and pole tide model values included in the GDR, are then used to compute the initial altimeter normal point residuals. Finally, the difference of these initial residuals with respect to the previously discussed reference ocean tide models provides the final residual measurement from which corrections to the ocean tide models are estimated.

In the following sub-sections, we discuss some of the important corrections mentioned in the previous paragraphs, and their significance for the modeling of ocean tides.

### 4.3. The TOPEX Orbit

The sea surface heights in the GDR are provided with respect to the NASA/GSFC POE. For this project, the sea surface heights were corrected to be with respect to the later and more accurate re-processed TOPEX orbits computed at UT/CSR. The new TOPEX orbits were computed with the updated geopotential model JGM3 which includes geopotential information from the SLR/DORIS tracking of the TOPEX satellite. More importantly, however, the orbits were computed with updated background ocean tide force model as compared to the original release POE.

In Bettadpur and Eanes (1994), it was shown that, much like the static geopotential, the radial orbit perturbations due to ocean tides were coherent with the tide height itself at each geographical location. The altimeter measurement being a radial distance measurements, the radial position errors in the orbit due to mismodeled ocean tides were inseparable from the altimeter measurement of the ocean tides. In fact, much of the differences between the first generation ocean tide models from T/P altimeter data (Eanes, 1994) and the older Geosat based C&R91 model were shown to be due to the inadequate modeling of the ocean tidal accelerations on the Geosat satellite (Bettadpur and Eanes, 1994).

While the long period, resonant effects of the mismodeled ocean tides could be adjusted into the estimates of the empirical acceleration parameters during the orbit determination process, it was shown (ibid.) that the non-resonant radial orbit errors, while retaining the same coherence with the ocean tides, could not be corrected by the same methods. The older TOPEX satellite orbits, including the earlier release POE placed on the GDR, were computed with background ocean tide force models based upon the NSW (Schwiderski, 1983) ocean tide heights. A comparison between the radial orbital effects of these and the newer T/P based models (Eanes, 1994) suggests that the earlier TOPEX orbits were in error up to 10 mm rms due to the errors of omission and commission in the earlier ocean tide force models. The principal effects, as might be expected were from the  $M_2$  harmonic, ranging up to 5 mm rms.

In the computation of the new TOPEX orbits, the background model was updated to use the preliminary T/P based ocean tide heights from the CSR 1.6 (Eanes 1994) model. Harmonics of the ocean tide height up to degree and order 20 for the principal 8 constituents  $Q_1, O_1, P_1, K_1$  and  $N_2, M_2, S_2, K_2$  were included in the background

model. Also included were complete degree and order 20 expansion of the  $M_m$  and  $M_f$  tides from the NSW model. It is expected that the rms radial orbit errors across all constituents does not exceed 5 mm in the new TOPEX orbits.

#### **4.4. Other Corrections**

As has been pointed out earlier, the body tides in the Diurnal and Semi-diurnal bands can be modeled to a high accuracy, so that we have chosen to treat body tides as corrections to be applied to the data. The only uncertainty in the modeling of the body tides is in the adopted values of  $h_2$  Love number. The body tide corrections used here were the same as provided on the GDR. The deformation of the solid Earth at each location was computed from a harmonic model.

The pole tide, having variability at annual and Chandler Wobble periods (14 months) does not significantly affect the models of the short period, Diurnal and Semi-diurnal tides. Corrections for the pole tide were used as provided on the GDR.

All other corrections, including the Wet/Dry Tropospheric and IB corrections, were based on the TOPEX/POSEIDON GDR models (Callahan, 1993).

## 5. OCEAN TIDE ESTIMATION

Having discussed the theoretical model for the ocean tides, as well as the corrections applied to the data, we now describe the parametrization and the least squares solution for the ocean tides from the T/P altimeter data.

### 5.1. The Data Distribution

The altimeter residuals, as described in the last section, were computed for the repeat cycles 1 through 89. The data from cycle 79 was not included because the POSEIDON altimeter data was not yet available. This dataset contains 10 second altimeter residual normal points for 872 days, or 2.4 years. Data from both TOPEX as well as the POSEIDON altimeter were included.

The global oceans between 66 degree North and 66 degree South, the region covered by the T/P satellite ground track, was divided into equi-angular grids of 3 degree by 3 degree in latitude and longitude. Note that with 3 degree square grids between 66 degree latitude bounds,  $n$  ranges from 1 through 5280. All the data were assigned to the appropriate bin depending upon the latitude and longitude of the measurement normal point. Reference point for each bin was taken to be the mid-point of the latitude and longitude limits for each bin.

### 5.2. The Model

Let  $\phi_i$  and  $\lambda_i$  denote the latitude and longitude of each measurement, made at epoch  $t_i$ . Further let  $n(i, j)$  denote the latitude and longitude dependent bin number for that data point. Further, let  $\phi_n$  and  $\lambda_n$  denote the bin reference latitude and longi-

tude. Within each bin, the residual normal point was modeled as follows.

$$\begin{aligned}
 y_{obs}(\phi_i, \lambda_i; t_i) = & b_n^0 + b_n^\phi (\phi_i - \phi_n) + b_n^\lambda (\lambda_i - \lambda_n) \\
 & + b_n^{\phi\phi} (\phi_i - \phi_n)^2 + b_n^{\phi\lambda} (\phi_i - \phi_n)(\lambda_i - \lambda_n) + b_n^{\lambda\lambda} (\lambda_i - \lambda_n)^2 \\
 & + C_n^a \cos A_a(t_i) + S_n^a \sin A_a(t_i) + \\
 & + C_n^{sa} \cos 2A_a(t_i) + S_n^{sa} \sin 2A_a(t_i) + \\
 & + C_n^1 \cos A_1(t_i) + S_n^1 \sin A_1(t_i) + \\
 & + \sum_{k=-1}^1 [ u_{n,k}^l a^l(t_i + k \Delta t) + v_{n,k}^l b^l(t_i + k \Delta t) ] \\
 & + \sum_{k: \text{even}}^4 [ u_{n,k}^d P_k^d(t_i) + v_{n,k}^d Q_k^d(t_i) ] \\
 & + \sum_{k: \text{even}}^4 [ u_{n,k}^s P_k^s(t_i) + v_{n,k}^s Q_k^s(t_i) ] \quad (22)
 \end{aligned}$$

The first line in Eq. 22 shows that a constant bias and mean sea surface slopes in the latitudinal and longitudinal directions were solved for each bin. The second line shows the model for the mean sea surface curvatures in the East, North and the East-North directions.

The next three lines shows the model for constant amplitude variations related to the Solar effects. The third and the fourth lines correspond to annual and semi-annual variations in the sea surface height, where

$$A_a(t_i) = 2\pi (T_i - 48988)/365.25 \quad (23a)$$

and  $T_i$  is the modified Julian date of the epoch of measurement, and 48988 refers to the MJD of Jan 1, 0h UTC. Inclusion of these parameters in model ensures that the constituents in the Diurnal and Semi-diurnal bands which have long period aliases due to T/P ocean sampling are not corrupted by the largely seasonal variations at the annual and semi-annual frequencies. Further, the fifth line corresponds to the exactly once per solar day variations, so that

$$A_1(t_i) = 2\pi \text{mod}(T_i, 1) \quad (23b)$$

These parameters corresponds to the solution for an ocean tide harmonic at the  $S_1$  frequency. Since the sea surface height variability at this frequency is driven by both

ocean tides as well as Solar heating variations, it is expected that the simultaneous solution for this harmonic along with the orthoweights for the entire Diurnal species will help separate the purely ocean tidal and Solar variations in the sea surface height.

The sixth line shows the parametrization of the long period tides. As can be seen on comparison with form of tide heights in Eq. 10, the long period species have been modeled with the conventional tidal response weights. The use of 48 hrs for the value of time lag implies that the six bin parameters  $u_{n,k}^l$  and  $v_{n,k}^l$  of the long period band response weights model the entire species, so that there is some redundance with the annual and semi-annual amplitudes described in the previous paragraph. This redundant parametrization is expected to help improve the models of long period ocean tides particularly at  $M_m$  and  $M_f$  frequencies.

The seventh and the eight lines show the parametrization of Diurnal and Semi-diurnal orthoweights, distinguished by the appropriate superscripts. These expressions are comparable to the Eqs. 5-6. The evaluation of the time dependent tidal arguments  $a(t)$  and  $b(t)$  for each species was carried out using the harmonic method, as written in Eq. 2b. The largest 97 amplitudes from the Cartwright and Edden (1973) harmonic decomposition of the tide generating potential were selected for evaluation of these functions. Of these 97, the Long-period band contained 20 constituents, the Diurnal band contained 44, and the Semi-diurnal band contained 33. The amplitudes  $H_k$  and the Doodson-Warburg phase factor  $\chi_k$  used in the evaluations are available on anonymous ftp. The tidal arguments in Eq. 2c were evaluated as described in McCarthy (1992), using arguments from Brown's Lunar Theory and Newcomb's theory for the Sun.

### 5.3. The Solution

As can be seen from Eq. 22, for each 3 degree bin, 20 parameters were solved from the altimeter normal point residuals. The partial derivatives of the observations with respect to each of the 20 parameters were accumulated into a 20 by 20 square linear system using the square-root-free Givens' rotations, so that

$$U_n \hat{x}_n = z_n \quad , \quad \hat{P}_n = (U_n^T D_n U_n)^{-1} \quad (24)$$

where  $\hat{x}_n$  denotes the solution for the 20 parameters of the bin number  $n$ ,  $U_n$  is a unit upper triangular matrix,  $D_n$  is a diagonal matrix, and  $\hat{P}_n$  is the *a posteriori* state error

covariance matrix.

For each bin, the pre-fit and post-fit altimeter normal point residual statistics, the linear predicted rms from the least squares solution, the estimate vector and the full covariance matrix were saved. Note finally that for the Diurnal and Semi-diurnal species, these solutions are to be regarded as corrections to the reference FES94.1 elastic ocean tide model.

#### **5.4. The Smoothed Solution**

Upon a visual inspection of the orthoweights of the Diurnal and Semi-diurnal ocean tides, it is easily seen that there is high frequency variability in the ocean tide orthoweights. The raw solutions must therefore be smoothed, as there is no reason to believe that the ocean tides are not smooth in the open oceans.

The smoothing of the raw elastic ocean tide corrections in these two species was carried out using a two-dimensional Gaussian smoother. This smoother had a Full-Width, Half-Maximum (FWHM) of 7 degrees.

Finally, the smoothed solution for the Diurnal and Semi-diurnal species was output on the same half degree grid as the orthoweights of the reference elastic ocean tide model. The sum of the reference model and the smoothed corrections provided the final elastic ocean tide model for the two species.

#### **5.5. Bottom Relative Ocean Tide : CSR 3.0**

The conversion from the elastic ocean tide to bottom-relative ocean tides requires the subtraction of ocean load tides, as indicated in Eq. 1. Using the same procedure as described Section 3.1 on the Reference Load Tide, the spherical harmonic decomposition of the orthoweights of the estimated elastic ocean tide were directly written as the sum of spherical harmonic decompositions of the load tide orthoweights and the bottom-relative tide orthoweights. As before, the load Love numbers were interpolated from the values tabulated by Farrell (1972). The scale factors in Eqs. 19 were applied to the decomposition of the elastic ocean tide in order to obtain the decomposition of the load tide. The load tide was then synthesized on the same grid as the estimated elastic ocean tide. Note that the load tide is now being derived from the estimated elastic ocean tide unlike the reference load tide model.

The difference between the estimated elastic ocean tide and the load tides is then the true bottom-relative ocean tide. The resulting half degree grid global maps of the orthoweights of the bottom-relative ocean tides in the Diurnal and Semi-diurnal species were called the **Model CSR 3.0**

## **6. MODEL CSR 3.0 : ASSESSMENTS**

Additional information and comparison with various other ocean tide models is given in Shum et al. (1997).

## REFERENCES

- Andersen, O.B. (1995), "Global ocean tides from ERS-1 and TOPEX/POSEIDON Altimetry," *JGR*, In press.
- Bettadpur, S.V. and R.J. Eanes (1994), "Geographical representation of radial orbit perturbations due to ocean tides: Implications for satellite altimetry," *JGR*, Vol. 99 (C12), pp 24,883-94.
- Callahan, P.S. (1993) "GDR Users handbook," JPL D-8944 Rev. A, Jet Propulsion Laboratory, Pasadena, CA.
- Canceil, P., R. Angelou and P. Vincent (1995), "Barotropic tides in the Mediterranean Sea from a finite element numerical model," *JGR*, In press.
- Cartwright, D.E., R.D. Ray, and B.V. Sanchez (1991), "Oceanic tide maps and spherical harmonic coefficients from Geosat altimetry," **NASA TM 104544**.
- Cartwright, D.E. and R.D. Ray (1990), "Oceanic tides from Geosat altimetry," *JGR*, Vol. 95 (C3), pp 3069-90.
- Cartwright, D.E. and A.C. Edden (1973), "Corrected tables of tidal harmonics," *Geophys. J. R. astr. Soc.*, Vol. 33, pp 253-64.
- Cartwright, D.E. and R.J. Tayler (1971), "New computations of the tide-generating potential," *Geophys. Jour. R. astr. Soc.*, Vol. 23, pp 45-74.
- Desai, S. and J.M. Wahr (1995), "Empirical ocean tide models estimated from TOPEX/POSEIDON data," Submitted to *JGR*.
- Eanes, R.J. (1994), "Diurnal and Semi-diurnal tides from TOPEX/POSEIDON altimetry," *EOS*, Trans. of AGU (Supplement), Vol. 75 (16), p 108.
- Eanes, R.J. and S.V. Bettadpur (1994), "Ocean tides from two years of TOPEX/POSEIDON altimetry," *EOS*, Trans. of AGU (Supplement), Vol. 75 (44), p 61.
- Farrell, W.E. (1972), "Deformation of the Earth by surface loads," *Revs. of Geophysics and Space Physics*, Vol. 10 (3), pp 761-97.

- Groves, G.W. and R.W. Reynolds (1975), "An orthogonalized convolution method of tide prediction," *JGR*, Vol. 80, No. 30, pp 4131-38.
- Le Provost, C. (1994), "A new in-situ reference data set for ocean tides," AVISO Altimetry Newsletter No. 3.
- McCarthy, D.D. (Ed.) (1992), "IERS Standards (1992)," **IERS Tech. Note 3**, Paris.
- Munk, W.H. and D.E. Cartwright (1966), "Tidal spectroscopy and prediction," *Phil. Trans. R. Soc. of London*, Vol. 259, Series A (Mathematical and Physical Sciences), pp 533-81.
- Ray, R.D. and B.V. Sanchez (1989), "Radial deformation of the Earth by oceanic tidal loading," **NASA TM 100743**.
- Schwiderski, E.W. (1983), "Atlas of ocean tidal charts and maps," Naval Surface Weapons Center, Dahlgren, Va.
- Shum, C.-K., P.L. Woodworth, O.B. Anderson, G. Egbert, O. Francis, C. King, S. Klosko, C. LeProvost, X. Li, J. Molines, M. Parke, R. Ray, M. Schlax, D. Stammer, C. Tierney, P. Vincent and C. Wunsch (1997), "Accuracy assessment of recent ocean tide models", *JGR*, To Appear.
- Tapley, B.D., D.P. Chambers, C.K. Shum, R.J. Eanes and J.C. Ries (1994), "Accuracy assessment of the large-scale dynamic ocean topography from TOPEX/POSEIDON altimetry," *JGR*, Vol. 90 (C12), pp24,605-18.
- Wahr, J.M. and T. Sasao (1981), "A diurnal resonance in the ocean tide and in the Earth's load response due to the resonant free 'core nutation'," *Geophys. J. R. astr. Soc.*, Vol. 64, pp 747-65.